Journal of Materials Chemistry

Dynamic Article Links

Cite this: *J. Mater. Chem.*, 2011, **21**, 16129

www.rsc.org/materials

PAPER

Flexible film materials from conjugated dye-modified polymer surfactant-induced aqueous graphene dispersions†

Horacio J. Salavagione,*[a] Gary Ellis,[a] José Luis Segura,[b] Rafael Gómez,[b] Gustavo M. Morales[c] and Gerardo Martínez[a]

Received 19th April 2011, Accepted 9th August 2011
DOI: 10.1039/c1jm11694k

A novel polymeric surfactant composed of a hydrophobic perylene dye covalently linked to hydrophilic poly(vinyl alcohol) (PVA) chains was employed to prepare stable aqueous dispersions of graphene. The presence of well-dispersed few layer graphene was demonstrated by UV-visible, Raman and fluorescence spectroscopy. This polymeric surfactant has an additional advantage in that it can be used to immobilize graphene within stable films that are transparent, flexible and easily processed. Indirect evidence of a strong interaction between perylene and graphene was obtained from the analysis of the physical properties of the polymer films. A complete loss of crystallinity and a remarkable reduction in segmental mobility manifested by an increase of around 50 °C in the glass transition temperature were observed. The imaginative molecular design of polymers covalently modified with planar aromatic molecules presents important opportunities in the development of new application possibilities of graphene.

Introduction

Graphene (Gr) is a recently discovered form of carbon consisting of a single layer of C atoms arranged in a honeycomb lattice. Despite being only one-atom thick, graphene is extremely strong and highly conductive; the charge carriers behave as massless Dirac fermions[1] making it ideal for high-speed electronics, photonics and beyond. Since its discovery graphene has shown much potential, but to date it has only been produced at a very small scale, limiting its potential measurement, understanding and development for medium- to large-scale applications. Several methods for the preparation of stable suspensions of graphene have been described, mainly consisting in the dispersion of graphite in organic solvents like NMP, DMF, *o*-dichlorobenzene, *etc.*[2,3] Although these low-yield methods have recently been improved,[4,5] at present the methods employed to produce larger quantities of graphene are based on thermal or chemical reduction of the defect-rich graphite oxide (GO), leading to products with limited properties when compared to those of the parent graphene. Recently, we developed a method to produce a dispersion of graphene in NMP with a concentration as high as 0.8 mg mL^{-1} by exfoliation of expanded graphite (EG) obtained under electrochemical reduction conditions that avoid the formation of GO.[6]

For some applications, for instance those involving biological or biomedical systems, graphene needs to be dispersible in water. However, graphene is clearly water insoluble due to its extended sp^2 carbon structure. In order to remedy this limitation Coleman *et al.*[7,8] and Hirsch *et al.*[9] have reported the use of surfactant molecules as key tools to induce water solubility of this highly hydrophobic material. In addition, natural polyphenols, *e.g.* tannic acid, have been used to disperse carbon nanotubes in water.[10] Although the validity of the use of natural or synthetic organic compounds to disperse carbon nanostructures has been recently demonstrated and the properties of the resultant solutions studied, especially in the case of carbon nanotubes,[11] this strategy does not ultimately lead to the preparation of functional materials in the form of homogeneous solid films that take advantage of the properties of each component.

The dispersion of graphene within polymeric matrices is clearly an attractive approach for practical exploitation since it combines the superlative properties of both components. Polymer-dispersed graphene films can find applications as flexible conductors, transparent conductive coatings for optoelectronic devices, and/or photonic materials. Recently we have reported the covalent functionalization of poly(vinyl alcohol) (PVA) with graphene laminates by esterification of PVA with GO and its subsequent reduction.[12] This material displayed a glass transition around 35 °C higher than that of the parent polymer, and was

[a]*Instituto de Ciencia y Tecnología de Polímeros, ICTP-CSIC, Dept. of Polymer Physics, Elastomers and Energy, c/Juan de la Cierva 3, 28006 Madrid, Spain. E-mail: horacio@ictp.csic.es; Fax: +34 915644853; Tel: +34 912587432*

[b]*Universidad Complutense de Madrid, Dpto. de Química Orgánica, 28040 Madrid, Spain*

[c]*Universidad Nacional de Río Cuarto, Dpto. de Química, Ruta 8, Km 631, 5800 Río Cuarto, Argentina*

† Electronic supplementary information (ESI) available: Description of the calculation of perylene units in PVAPery, additional Raman spectra showing the perylene bands, Raman map analysis, and some images of the cast film. See DOI: 10.1039/c1jm11694k

found to be completely amorphous. However, it did not manifest measurable conductivity values. This can be explained by several reasons: (i) the low degree of graphene incorporation due to steric hindrance, (ii) their attachment to the polymeric chain that reduces electron mobility in terms of hopping between graphene laminates, and/or (iii) the inefficiency of the reduction reaction when GO is linked to the polymer that leads to a product containing more oxygen defects than usual. Similarly, as mentioned earlier, the direct compatibilization of hydrophobic graphene with polar polymers is also impossible *per se*. However, the functionalization of these polymers with aromatic molecules that can directly interact with graphene emerges as an interesting alternative, one example being the present case of perylene derivatives.

Finally, in relation to the importance of dispersing graphene both in water and in polymeric matrices, especially in those useful for biological applications, we consider that a polymer surfactant may exert a dual role by both inducing the efficient dispersion of graphene in water and by providing a mechanically stable environment for the formation of graphene-containing films. PVA emerges as an ideal polymeric material for this purpose because it is biocompatible, has excellent film forming ability as well as high oxygen barrier properties.

Recently, we studied the esterification of PVA with a perylene derivative.[13] After esterification of PVA with (*N*-(carboxyphenyl)-*N*′-(8-pentadecyl)perylene-3,4:9,10-bis(dicarboximide)) (PDI) we obtained a new polymer (denominated PVAPery) that retained the solubility of the parent PVA. In this paper we report the use of the polymer PVAPery to homogeneously disperse graphene in water. The π–π stacking interaction between the perylene moieties immobilized in PVA and the graphene is responsible for the improved solubility. In addition, coagulation of the PVAPery/Gr system produces solid products with different properties with respect to those of modified PVA, including improved mechanical and electrical properties.

Experimental section

Preparation of expanded graphite (EG)

EG was prepared using the method reported in ref. 6. Briefly, a graphite electrode (SIGRAFLEX®, SLG-Carbon S.E., Wiesbaden, Germany) was subjected to double potential step experiments to produce intercalated graphite. A potential of 0 V was initially applied for 10 s followed by a perturbation potential of −1 V for 5 minutes. The potential was finally reset to the original value for 10 s. The final EG was prepared by microwave treatment of the intercalated graphite for 5–10 seconds by using a conventional microwave oven (2.4 GHz) at a nominal power of 800 W under argon atmosphere.

Preparation of PVAPery

The esterification of PVA with PDI was undertaken according to ref. 13. Appropriate amounts of PDI and PVA were suspended in DMSO. The suspension was gently stirred and maintained at 70 °C under nitrogen for 2 h. Then a solution of *N*,*N*-dicyclohexylcarbodiimide (DCC) and 4-dimethylaminopyrydine (DMAP) in dimethylsulfoxide (DMSO) was added, and the resulting mixture was stirred at 40 °C for 3 days. The addition of methanol in abundance with vigorous stirring provoked coagulation of the product. The resulting solid was filtered, washed with methanol and dried at 50 °C under vacuum for 24 h. The product was then redissolved in hot water and centrifuged at a high speed (16 000 rpm) for 1 h to eliminate any remaining unreacted PDI, and the colored supernatant solution was subsequently coagulated with methanol. This procedure was repeated twice.

Preparation of PVAPery/Gr

A PVAPery sample with 15 wt% of perylene derivative was employed. A solution of 5×10^{-4} M of perylene in water was prepared. Then 5 mg of expanded graphite was added to the solution, stirred for 5 minutes and then treated with an ultrasonic probe for 20 min (applied energy *ca.* 19 kJ). It has been demonstrated that the ultrasonic treatment conditions are critical since a minimum period of time is required in order to ensure exfoliation without provoking irreversible damage to the sp^2 network.[5] In order to eliminate the non-interacting graphene and other graphitic materials, the solution was allowed to precipitate for 72 h and the precipitate discarded. Only the supernatant dispersion was used in the subsequent experiments. Although we also studied the case for more dilute solutions of PVAPery, significant changes were only observed at concentrations higher than 5×10^{-4} M.

PVAPery/G films were prepared by controlled evaporation of aqueous solution at 50 °C.

Characterization

UV-vis absorption spectra were recorded from aqueous dispersions (pH = 7) on a Perkin–Elmer Lambda 40 spectrophotometer and photoluminescence spectra on a JASCO FP6200 spectrometer.

Raman measurements were undertaken in the Raman Microspectroscopy Laboratory of the Characterization Service in the Institute of Polymer Science & Technology, CSIC. A Renishaw InVia Reflex Raman system (Renishaw plc, Wotton-under-Edge, UK) was used, employing a grating spectrometer with a Peltier-cooled charge-coupled device (CCD) detector coupled to a confocal microscope. All spectra were processed using Renishaw WiRE 3.2 software. The Raman scattering was excited using an Argon ion laser wavelength of 514.5 nm. The laser beam was focused on the sample with a 100× microscope objective (NA = 0.85), with a laser power at the sample of <2 mW.

The crystallization and melting behaviour were investigated by differential scanning calorimetry (DSC) using a Mettler TA4000/DSC30 apparatus. The experiments were undertaken in a nitrogen atmosphere using samples with a mass of ∼5 mg sealed in aluminium pans. The samples were heated from the solid state at room temperature to the melt at 240 °C, maintained at this temperature for 5 minutes to eliminate any thermal history, then cooled to room temperature and subsequently heated once more to 240 °C. Heating and cooling rates of 10 °C min^{-1} were used in all cases. The transition temperatures were taken as the peak maxima in the calorimetric curves. The degree of crystallinity (X_c) was calculated from the ratio $\Delta H_a/\Delta H_u$,

where ΔH_a is the apparent heat of fusion calculated from the integrated area of the melting peak, and ΔH_u the melting enthalpy for 100% crystalline PVA,[14] 161.6 J g^{-1}.

Scanning electron microscopy microphotographs of the EG were collected using a Philips XL30 SEM. The samples were coated with around 5 nm Au/Pd overlayer to avoid charging during electron irradiation.

Results and discussion

In this study we employed the EG obtained by electrochemical intercalation at −1 V and subsequent microwave-assisted expansion of a 1-mm-thick laminated graphite foil of lateral dimensions 8 mm × 15 mm.[6] As detailed in the Experimental section, the EG was sonicated in an aqueous solution of PVAPery (pH = 7). After 72 hours a solid precipitate was observed at the bottom of the vial, but the color of the supernatant was seen to vary from that of the PVAPery solutions. The supernatant was separated and on illumination with a laser beam it demonstrated the Tyndall scattering effect (Fig. 1a), confirming the presence of small particles of dispersed graphene.

Examination of the absorption spectra of the PVAPery/Gr dispersions further confirmed the presence of graphene flakes (Fig. 1b). It is important to indicate that the spectrum was baseline-corrected to eliminate the influence of scattering, and the peaks of the polymeric surfactant were subtracted to visualize only the features of the dispersed graphene.[9] The resulting absorption spectrum (Fig. 1b) shows a peak with a maximum at 275 nm attributed to the π-conjugated network within the graphene nanosheets[15–17] resembling the results obtained by Hirsch and colleagues.[9] Using the experimental absorption coefficient for graphene dispersion in surfactant solutions (1390 L g^{-1} m^{-1}) reported by Lotya *et al.*[7] we calculated the concentration of the dispersed material to be approximately 0.021 g L^{-1}. Unlike Lotya *et al.* who used a totally ionized surfactant in water (sodium dodecylbenzene sulfonate, SDBS), our surfactant dissolved in water *via* hydrogen bonding and the hydroxyl groups are not ionized. However, the concentration of dispersed graphene was calculated from a region of the absorption spectra that has no contribution from either SDBS or PVAPery in ref. 7 and in this work, respectively. Therefore, despite the differences in ionic strength[11] of both surfactants in terms of attraction/repulsion with graphene laminates, the absorption coefficient at 660 nm from ref. 7 can be used without introducing any significant error.

As shown in the earlier work,[13] the perylene-modified polymeric compound employed to disperse graphene has a characteristic emission spectrum (Fig. 1c). The study of the emission spectrum of PVAPery/Gr can provide us with more information about the presence of graphene and its interaction with the surfactant. The absorption spectrum of perylene shows absorption bands that can be attributed to non-associated and self-assembled perylene.[18] Although these terms are used for solutions of perylene molecules, it can be extended to perylene bound to PVA due to the dynamics of PVA chains in solutions. We irradiated samples at the wavelength corresponding to non-associated perylene (490 nm) to analyze the influence of dispersed graphene. A slightly lower emission intensity was observed for PVAPery/Gr suggesting that the concentration of non-associated perylene diminished as a consequence of its interaction with graphene (Fig. 1c). One possible explanation for this decrease in the emission intensity may be a resonance energy transfer from the excited state of perylenebisimide[19–21] to graphene.[22] Single layer graphene is characterized by a linear band dispersion around the corner of the Brillouin zone (K and K' points)[23] and a nearly constant optical absorption. Thus, resonance energy transfer from different fluorophores to single and few-layer graphene is expected to occur[24] since these systems exhibit broad absorption across the visible spectral range. Regardless of the quenching mechanism, the observed magnitude of the effect was to be expected because, whereas graphene has been previously demonstrated to strongly quench fluorescence,[25,26] the overall concentration of dispersed graphitic materials, and as such the absolute concentration of single layer graphene, is relatively low. Consequently, for such low concentration we may consider the overall quenching effect as significant.

In order to obtain more evidence on the nature, thickness and quality of the graphene in the aqueous PVAPery/Gr dispersions, Raman spectra were recorded after careful deposition *via* spin-coating onto a silicon wafer covered with a thin (90 nm) SiO_2 layer. Carbonaceous flakes could be easily located on the substrate and presented lateral dimensions of up to 10 μm. However, one of the main difficulties encountered in the analysis of the graphene layers was the presence of the polymer. This made it impossible to perform useful AFM measurements, and

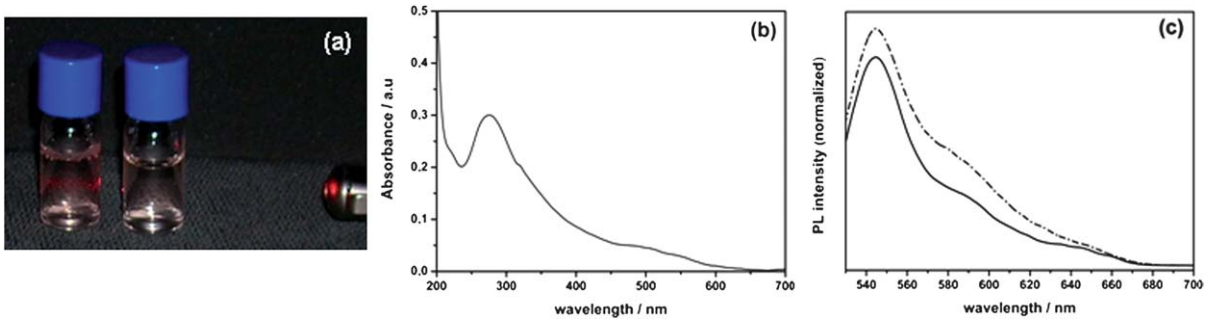

Fig. 1 Optical characterization of PVAPery/Gr. (a) Photo showing the Tyndall scattering effect (He–Ne laser, 632.8 nm) in PVAPery/Gr due to dispersed graphene (left vial) and the transparent pure solution of PVAPery (right vial). (b) Absorption spectrum of PVAPery/Gr after baseline correction and perylene peak subtraction. (c) Emission spectra of PVAPery (5×10^{-4} M, dot) and PVAPery/Gr (solid). $\lambda_{exc} = 490$ nm. The concentration of PVAPery is the same in both cases.

resulted in a significant deterioration in the contrast in electron microscopy. The Raman measurements on the graphene flakes were also not without some difficulties due to a high fluorescent background and the superposition of resonance Raman scattering (RRS) signals from the perylene moiety in the polymer host (see ESI†), since the vibrations excited at the laser wavelength employed here are in resonance with the electronic transitions of the dye molecule. Although the quantity of perylene is very low in the system the RRS intensity is sufficient to be observed in the Raman spectra.[22,27,28]

Fig. 2 shows a visible image obtained from a typical surface deposit, and Raman spectra recorded from two points on the sample. Spectrum 1 corresponds to a clearly visible flake in the region between 1100 and 1700 cm^{-1} where the G mode can be clearly identified, and spectrum 2 to the surrounding material where bands corresponding to the RRS spectrum of the perylene moiety are seen. Raman images were constructed from (i) the integrated intensity of the A_g mode of perylene at around 1300 cm^{-1} and (ii) from the integrated intensity between 1500 and 1650 cm^{-1} that includes both the graphene G-mode and a doublet also corresponding to the perylene moiety at around 1572 and 1587 cm^{-1}. Chemometric analysis was employed to further analyze the mapping data, and confirmed the identification and discrimination between the perylene RRS bands and the graphene flakes (see ESI†).

Evidence for few layer (FLG) and multilayer graphene was found in the dispersed particles by analysis of the second-order 2D peaks arising from the zone boundary phonons[29–31] with the lowest thicknesses estimated between 2 and 4 layers.[23,30–35] Fig. 3 shows a series of example Raman spectra recorded from different flakes with different layer thicknesses.

One important observation was that the experimental procedure employed to disperse graphene in these polymeric solutions does not have a negative influence on the carbon material integrity. It should be pointed out that in all the spectra obtained the D-band intensity, which provides an indication of the number of defects in the carbon network, remains very low, and in some cases was almost imperceptible, albeit the overlap with the RRS signals from perylene makes it difficult to make a precise evaluation. The fact that this aqueous dispersion

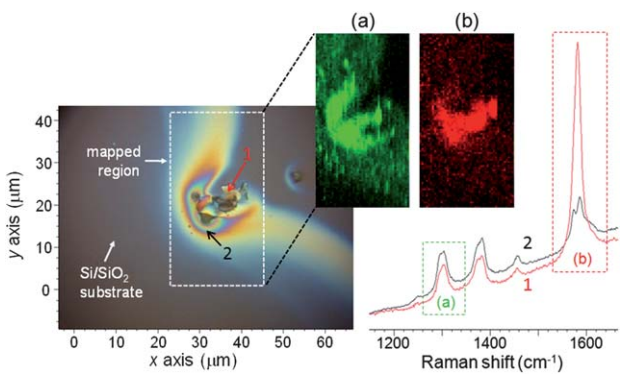

Fig. 2 Visible image of a typical deposit of PVAPery/Gr on a Si/SiO_2 substrate, and Raman spectra recorded from positions 1 and 2 (marked). Raman maps of the area defined by the white box correspond to (a) the integrated area of the peak at around 1300 cm^{-1} and (b) the integrated intensity of the 1500–1650 cm^{-1} region.

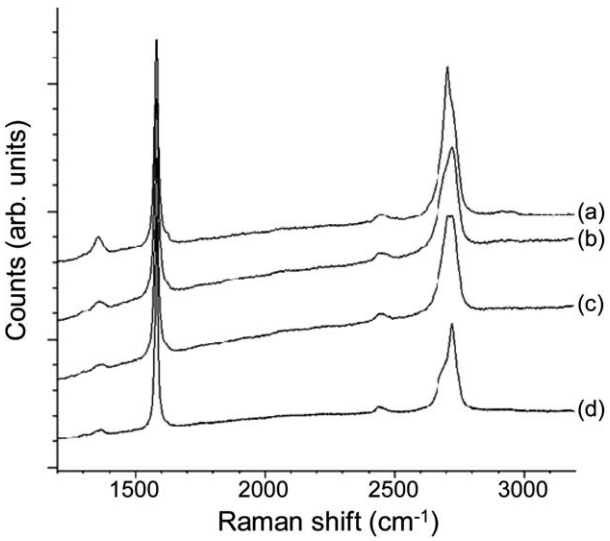

Fig. 3 Raman spectra obtained from different flakes showing the presence of few-layer graphene (FLG). The following layer thicknesses were estimated using already developed band deconvolution methods[29,30,35] (a) 2, (b) 5, (c) 4 and (d) >10.

method maintains the integrity of the sp^2 structure indicated that high-quality FLG could be obtained. It is clear that the method reported here can be optimized to obtain less polydisperse products and ultimately increase the quantity of single layer graphene.[36]

Once the ability of the polymeric surfactant to disperse graphene was confirmed and the solution properties studied, we wanted to go one step further and prepare a final solid material with potential functional properties. This was viable in our case due to the polymeric dispersing agent, but is impossible when using single organic molecules as surfactants. The PVAPery polymeric surfactant surrounding the graphene can act as a vehicle for the preparation of homogeneous films with the processing advantage of the polymer and the outstanding properties of graphene, where the perylene effectively compatibilizes the interface. The material could be cast to generate a very transparent, flexible film (Fig. S5†). Scale-up is currently underway, and the evaluation of the mechanical properties will be reported at a later date.

Scanning electron microscopy (SEM) images from the fracture surfaces of thin film samples show a well-dispersed, well-aligned distribution of graphene sheets in the PVAPery matrix (PVA image is shown for comparison), mostly around 10 μm in length with an overall thickness of around 50 nm with few aggregates (Fig. 4). This quite uniform distribution may be promoted by effective graphene-perylene interactions. In order to verify these and analyze their effect on the properties of the host polymer we employed differential scanning calorimetry (DSC).

The crystallization and melting behaviours were analyzed by cooling all samples from the melt to 30 °C at a rate of 10 °C min^{-1} and subsequently heating to 240 °C at the same rate (Fig. 5). A PVAPery sample with a perylene fraction (F_p) in the polymeric surfactant of 0.16–0.18 was used.[13] Compared to neat PVA[13,14] this sample showed a very broad melting endotherm (T_m) with a maximum at 202 °C, and a degree of crystallinity (X_c)

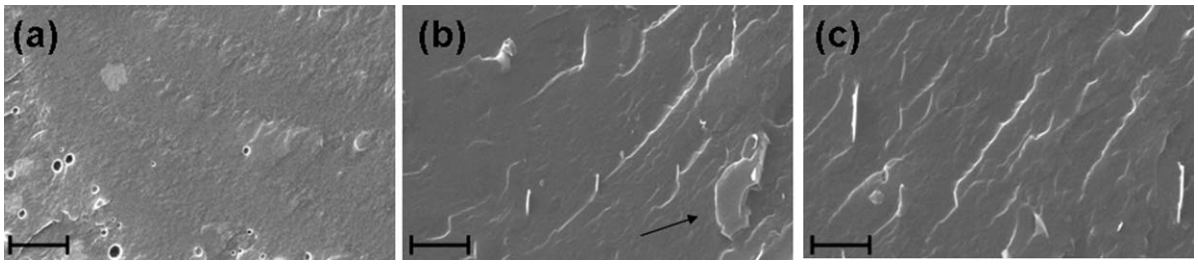

Fig. 4 SEM images of a fracture section of PVA (a) and PVAPery/Gr at different magnifications (b and c). The arrow in (b) shows a flake of 15 μm long and 4.5 μm wide and folded in one corner. Other edge-on flakes can also be seen in (b) and (c). Scale bars in (a) and (b) = 10 μm, and (c) = 5 μm.

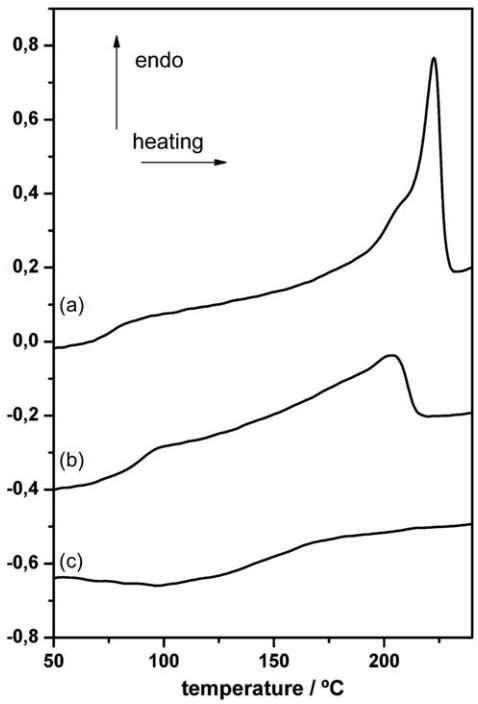

Fig. 5 DSC heating scans at 10 °C min^{-1} of (a) pure PVA, (b) PVAPery and (c) PVAPery/Gr.

calculated for PVA of around 20% (Fig. 5b), somewhat lower than that of the neat polymer host, which had a value of about 50% for an identical thermal history (Fig. 5a). A higher glass transition temperature (T_g) between 90 and 92 °C was also observed with a similar scale with respect to onset and endset temperature values. Clearly some variations in the crystalline parameters and the T_g of the host polymer in the presence of graphene were to be expected.[12,37,38] However, the PVAPery/Gr sample showed a radically different thermal behaviour (Fig. 5c). In the DSC heating scan the peak corresponding to the melting endotherm completely disappeared, implying that the presence of graphene totally inhibits crystal formation in the semicrystalline PVA polymer. A similar amorphous material was obtained by esterification of PVA with GO that gave a product with huge graphitic laminates covalently bonded to the PVA matrix,[12] and Yang *et al.* recently obtained a similar amorphous material in PVA/graphene nanocomposites produced by reduction of GO with hydrazine in an aqueous solution of PVA.[38] However, in the present case the graphene sheets are not covalently bonded to the polymer, moreover it appears that their interaction with the perylene moieties in PVAPery is sufficiently strong to inhibit crystal formation in samples prepared with the same thermal history.

Furthermore, in our case the T_g is observed to broaden significantly and shift to much higher temperature, by more than 50 °C with respect to that of PVAPery. Such a dramatic change in T_g has not been previously reported for this kind of polymeric system. Further, the increase is far superior to the values obtained in the previously cited examples.[12,38] The heterogeneous nature of the transition occurring over a broad temperature range suggests that in this case the proximity of graphene to the polymer chains through an effective non-covalent association mechanism not only prevents crystallization but also inhibits the segmental freedom of movement of the polymer chains, impeding reordering. The consequence of this is an increase in stiffness of the polymer that can certainly be an interesting improvement in the materials properties in terms of tensile modulus and dimensional stability. Also the complete elimination of crystallinity can have a positive effect on the transparency of the material. Such improvements may be fundamental when considering this type of materials for device applications such as solar cells, flexible electronics, *etc.*

Considering the composition of PVAPery used in this work and the average molecular weight of the PVA employed (~90 000 g mol^{-1}) we can roughly estimate the presence of a mean value of around 19.8 perylene units along each polymer chain (ESI†). The perylene moiety slightly alters the overall segmental mobility of a specific chain length, reflected in the

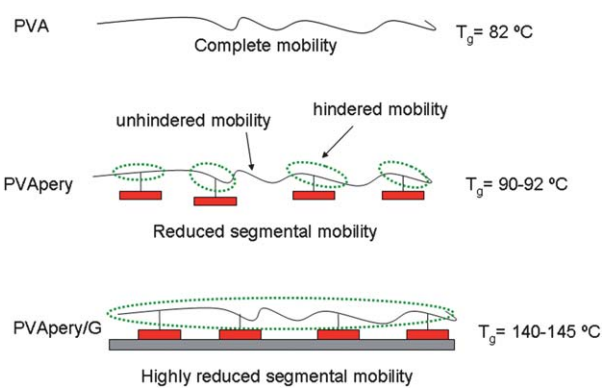

Fig. 6 Schematic representation illustrating the changes in the PVA mobility after covalent modification with perylene and subsequent interaction with graphene.

reduction of crystallizable segment lengths in the polymer (Fig. 6). Further, when the relatively huge graphene laminates are present in the polymer, although in low concentration as calculated by UV-Vis, they can interact with several perylene groups along the same chain, or in other chains, producing an effective immobilization of longer polymer segments at the graphene surface, resulting in a very broad glass transition temperature and the total absence of crystallization (Fig. 6).

Some preliminary tests on the conductivity of the material were made. Although the reduced dimensions of the samples did not allow the use of a four-probe system, a high impedance multimeter was employed in order to obtain a measure of the insulating or conducting character of the product. With the two contacts placed 3 mm apart on 500-μm-thick films, a resistance value of *ca.* 1.2×10^6 Ω was observed. Although, *a priori* this resistance value is high, sufficient conductivity was observed to suggest that conductive materials could be obtained using this procedure. Naturally the perylene modified PVA behaves as an insulating material. Compared to systems where graphene is covalently bound to PVA,[12] which is an insulating material, the conductivity of PVAPery/Gr can be attributed to a higher concentration of graphene as well as to the better quality of the graphene used here. In the case of the covalently bound system, GO, that has poorer properties than expanded graphite, is employed. Additionally, the location on the graphene laminates where the PVA is linked is actually a defect that disrupts the sp^2 network even though the final product is reduced.

More detailed studies of the structure and properties of PVAPery/Gr nanocomposites are currently underway in our laboratory, including scale-up of the materials preparation in order to perform mechanical and electrical properties testing under standard conditions, the results of which will be reported at a later date.

Conclusions

We have demonstrated the effective use of a polymeric surfactant to induce the solubility of graphene in water. The polymeric surfactant also allows us to prepare stable and homogeneous solid films with the promise of viable functional properties. The presence of graphene dramatically altered the final properties of the material due to efficient PVA-to-graphene interactions driven by the perylene groups. This study is a starting point that can be extended to other polymeric matrices with improved film-forming ability and solubility in a broad range of organic solvents. As demonstrated here, the imaginative molecular design of polymers covalently modified with aromatic planar molecules could provide an advancement to the potential and exploitation of graphene-based nanocomposites. This route emerges as a pioneering tool to produce flexible graphene films.

Acknowledgements

Financial support was provided by the Spanish Ministry of Science and Innovation (MICINN) *via* Projects MAT2009-09335, MAT-2010-21070-C02-01 and CTQ2010-14982. H.J.S. thanks the MICINN for a Ramón y Cajal Research Fellowship. Finally, the authors wish to thank Isabel Muñoz of the ICTP Characterization Service for obtaining some of the Raman spectra.

Notes and references

1 K. S. Novoselov, A. K. Geim, S. V. Morozov, D. Jiang, M. I. Katsnelson, I. V. Grigorieva, S. V. Dubonos and A. A. Firsov, *Nature*, 2005, **438**, 197.
2 Y. Hernandez, V. Nicolosi, M. Lotya, F. M. Blighe, Z. Sun, S. De, I. T. Mcgovern, B. Holland, M. Byrne, Y. K. Gun'ko, J. L. Boland, P. Niraj, G. Duesberg, S. Krishnamurthy, R. Goodhue, J. Hutchison, V. Scardaci, A. C. Ferrari and J. N. Coleman, *Nat. Nanotechnol.*, 2008, **3**, 563.
3 C. E. Hamilton, J. R. Lomeda, Z. Sun, J. M. Tour and A. R. Barron, *Nano Lett.*, 2009, **9**, 3460.
4 X. Wang, P. F. Fulvio, G. A. Baker, G. M. Veith, R. R. Onocic, S. M. Mahurin, M. Chi and S. Dai, *Chem. Commun.*, 2010, **46**, 4487.
5 U. Khan, A. O'Neill, M. Lotya, S. De and J. N. Coleman, *Small*, 2010, **6**, 864.
6 G. M. Morales, P. Schifani, G. Ellis, C. Ballesteros, G. Martínez, C. Barbero and H. J. Salavagione, *Carbon*, 2011, **49**, 2809.
7 M. Lotya, Y. Hernandez, P. J. King, R. J. Smith, V. Nicolosi, L. S. Karlsson, F. M. Blighe, S. De, Z. Wang, I. T. McGovern, G. S. Duesberg and J. N. Coleman, *J. Am. Chem. Soc.*, 2009, **131**, 3611.
8 M. Lotya, P. J. King, U. Khan, S. De and J. N. Coleman, *ACS Nano*, 2010, **4**, 3155.
9 J. M. Englert, J. Röhrl, C. D. Schmidt, R. Graupner, M. Hundhausen, F. Hauke and A. Hirsch, *Adv. Mater.*, 2009, **21**, 4265.
10 C. A. Backes, C. D. Schmidt, F. Hauke, C. Böttcher and A. Hirsch, *J. Am. Chem. Soc.*, 2009, **131**, 2172.
11 D. Lin, N. Liu, K. Yang, L. Zhu, Y. Xu and B. Xing, *Carbon*, 2009, **47**, 2875.
12 H. J. Salavagione, M. A. Gómez and G. Martínez, *Macromolecules*, 2009, **42**, 6331.
13 H. J. Salavagione, G. Martínez, R. Gómez and J. L. Segura, *J. Polym. Sci., Part A: Polym. Chem.*, 2010, **48**, 3613.
14 *Polymer Data Handbook*, ed. J. E. Mark, Oxford University Press, 1998, p. 899.
15 Y. Zhou, Q. Bao, L. A. L. Tang, Y. Zhong and K. P. Loh, *Chem. Mater.*, 2009, **21**, 2950.
16 D. Li, M. B. Muller, S. Gilje, R. B. Kaner and G. G. Wallace, *Nat. Nanotechnol.*, 2008, **3**, 101.
17 T. Eberlein, U. Bangert, R. R. Nair, R. Jones, M. Gass, A. L. Bleloch, K. S. Novoselov, A. Geim and P. R. Briddon, *Phys. Rev. B: Condens. Matter Mater. Phys.*, 2008, **77**, 233406.
18 W. Wang, J. J. Han, L. Q. Wang, L. S. Li, W. J. Shaw and A. D. Q. Li, *Nano Lett.*, 2003, **3**, 455.
19 C. C. Hofmann, S. M. Lindner, M. Ruppert, A. Hirsch, S. A. Haque, M. Thelakkat and J. Köhler, *J. Am. Chem. Soc.*, 2009, **131**, 4819.
20 R. Gómez, D. Veldman, R. Blanco, C. Seoane, J. L. Segura and R. A. J. Janssen, *Macromolecules*, 2007, **40**, 2760.
21 E. E. Neuteboom, S. C. J. Meskers, P. A. Van Hal, J. K. J. Van Duren, E. W. Meijer, R. A. J. Janssen, H. Dupin, G. Pourtois, J. Cornil, R. Lazzaroni, J. L. Bredas and D. Beljonne, *J. Am. Chem. Soc.*, 2003, **125**, 8625.
22 N. V. Kozhemyakina, J. M. Englert, G. Yang, E. Spiecker, C. D. Schmidt, F. Hauke and A. Hirsch, *Adv. Mater.*, 2010, **22**, 5483.
23 A. H. Castro Neto, F. Guinea, N. M. R. Peres, K. S. Novoselov and A. K. Geim, *Rev. Mod. Phys.*, 2009, **81**, 109.
24 Z. Chen, S. Bericaud, C. Nuckolls, T. F. Heinz and L. E. Brus, *ACS Nano*, 2010, **4**, 2964.
25 J. Kim, L. J. Cote, F. Kim and J. Huang, *J. Am. Chem. Soc.*, 2010, **132**, 260.
26 S. Essig, C. W. Marquardt, A. Vijayaraghavan, M. Ganzhorn, S. Dehm, F. Hennrich, F. Ou, A. A. Green, C. Sciascia, F. Bonaccorso, K. P. Bohnen, H. V. Lohneysen, M. M. Kappes, P. M. Ajayan, M. C. Hersam, A. C. Ferrari and R. Krupke, *Nano Lett.*, 2010, **10**, 1589.
27 K. Ackers, R. Aroca, A. M. Hor and R. O. Loutfy, *Spectrochim. Acta, Part A*, 1988, **44**, 1129.
28 G. Salvan, S. Silaghi, M. Friedrich, C. Himcinschi and D. R. T. Zahn, *J. Optoelectron. Adv. Mater.*, 2006, **8**, 604.

29 A. C. Ferrari, J. C. Meyer, V. Scardaci, C. Casiraghi, M. Lazzeri, F. Mauri, S. Piscanec, D. Jiang, K. S. Novoselov, S. Roth and A. K. Geim, *Phys. Rev. Lett.*, 2006, **97**, 187401.
30 D. Graf, F. Molitor, K. Ensslin, C. Stampfer, A. Jungen, C. Hierold and L. Wirtz, *Nano Lett.*, 2007, **7**, 238.
31 Z. H. Ni, H. M. Wang, J. Kasim, H. M. Fan, T. Yu, Y. H. Wu, Y. P. Feng and Z. X. Shen, *Nano Lett.*, 2007, **7**, 2758.
32 M. S. Dresselhaus, A. Jorio, M. Hofmann, G. Dresselhaus and R. Saito, *Nano Lett.*, 2010, **10**, 751.
33 A. C. Ferrari, *Solid State Commun.*, 2007, **143**, 47.
34 Y. Hao, Y. Wang, L. Wang, Z. Ni, Z. Wang, R. Wang, C. K. Koo, Z. Shen and J. T. L. Thong, *Small*, 2010, **6**, 195.
35 A. Gupta, G. Chen, P. Joshi, S. Tadigadapa and P. C. Eklund, *Nano Lett.*, 2006, **6**, 2667.
36 (*a*) A. A. Green and M. C. Hersam, *Nano Lett.*, 2009, **9**, 4031; (*b*) A. A. Green and M. C. Hersam, *J. Phys. Chem. Lett.*, 2010, **1**, 544.
37 H. J. Salavagione, G. Martínez and M. A. Gómez, *J. Mater. Chem.*, 2009, **19**, 5027.
38 X. Yang, L. Li, S. Shang and X. M. Tao, *Polymer*, 2010, **51**, 3431.